



# Anisotropy in Fourier space optical memory effect correlations

Niall Byrnes<sup>1</sup>, and Matthew R. Foreman<sup>1,2</sup>\*

<sup>1</sup>*School of Electrical and Electronic Engineering,*

*Nanyang Technological University, 50 Nanyang Avenue, Singapore 639798*

<sup>2</sup>*Institute for Digital Molecular Analytics and Science, 59 Nanyang Drive, Singapore 636921*

(Dated: May 6, 2026)

We investigate anisotropy in Fourier-domain speckle correlations associated with the optical memory effect in disordered scattering media. Within a single scattering framework, we show that while the conventional memory effect constrains transverse wavevector shifts, the correlation strength also depends non-trivially on differences in the axial wavevector components. Our theory is supported by numerical simulations of a three-dimensional, single scattering medium, which show excellent agreement with theory. We extend the analysis to pseudo-correlations, demonstrating that analogous anisotropic behavior arises in the conjugate memory effect. Our results highlight the often neglected role of axial disorder in scattered field correlations.

The optical memory effect describes a fundamental correlation exhibited by speckle patterns produced by waves propagating through complex scattering media under small angular tilts of the incident field [1]. Since its initial discovery, substantial effort has been devoted to understanding its physical origin [2], as well as its connections to other key aspects of wave propagation in disordered media, including time-reversal symmetry [3], polarization [4], and scattering eigenchannels [5]. The memory effect is now a central tool in speckle correlation imaging [6], and has found broader application in, for example, optical fiber communications [7]. A wide range of generalizations to the memory effect have also been established, demonstrating that speckle correlations persist under more general angular tilts [8], combinations of shifts and tilts of the incident field [9], and other types of transformations, such as frequency shifts [10], axial displacements [11], and rotations [12].

A scattered field emerging from a complex medium is typically expressed as a sum of many partial fields, each associated with a distinct sequence of scattering events within the medium. The statistical properties of the scattered fields are obtained by averaging appropriate combinations of these partial fields over different physical realizations of the underlying disorder. The memory effect in particular arises as a constructive interference phenomenon when averaging over the transverse spatial dimensions of the scattering medium [13]. Averaging over the axial (longitudinal) disorder, on the other hand, is typically ignored. In this work, we show that consideration of the axial disorder yields a residual correlation function in the Fourier domain that is non-uniform with respect to the directions of the incident and scattered wavevectors, even when the memory effect condition is satisfied. We explain this phenomenon theoretically and present results from numerical simulations validating our theory.

We consider a three-dimensional slab centered at the origin with spatial extents  $L_x, L_y$ , and  $L_z$  along the

Cartesian axes. We define the  $x$  and  $y$  axes as transverse directions, the  $z$  axis as the axial direction, and assume that  $L_x, L_y \gg L_z$ . The interior of the slab is populated with  $N$  randomly distributed point scatterers. The slab is illuminated by a monochromatic, unit-amplitude plane wave  $E_i(\mathbf{r}) = \exp(i\mathbf{k}_i \cdot \mathbf{r})$ , with incident wavevector  $\mathbf{k}_i$ . Note that while we neglect polarization for simplicity, our final results remain valid in a full vectorial treatment [14]. In an arbitrary measurement plane  $z = z_m$  on either side of the slab, the scattered field can be decomposed into a spectrum of plane waves [15]. Assuming that  $L_z$  is smaller than the medium's scattering mean free path, the plane wave component of the scattered field propagating with wavevector  $\mathbf{k}_j$  has complex amplitude given by [13]

$$\tilde{E}_{ji} \sim \sum_{n=1}^N f_n(\mathbf{k}_j, \mathbf{k}_i) \exp(i\mathbf{r}_n \cdot [\mathbf{k}_i - \mathbf{k}_j]), \quad (1)$$

where  $n$  enumerates the scatterers,  $\mathbf{r}_n$  is the location of the  $n$ 'th scatterer, and  $f_n$  is a form factor for the  $n$ 'th scatterer.

The optical memory effect manifests in the field correlation  $C_{ijuv} = \langle \tilde{E}_{ji} \tilde{E}_{vu}^* \rangle$ , where  $u$  and  $v$  denote an additional pair of incident and scattered plane wave directions, and the average is taken over the ensemble of realizations of the scattering medium. For simplicity, we consider the case of a monodisperse collection of identical scatterers whose positions are independent and identically distributed according to a common density function  $p$ , which is non-zero only within the slab. Under these assumptions,  $C_{ijuv}$  reduces to

$$C_{ijuv} \sim \langle \exp(i\mathbf{r}_p \cdot [\mathbf{k}_i - \mathbf{k}_j - \mathbf{k}_u + \mathbf{k}_v]) \rangle, \quad (2)$$

which can be identified as the characteristic function of the spatial distribution of the scatterers, evaluated at  $\mathbf{q} = \mathbf{k}_i - \mathbf{k}_j - \mathbf{k}_u + \mathbf{k}_v$  [16]. We assume that the slab is homogeneous in the transverse coordinates and that, for  $\mathbf{r}$  inside the slab,  $p(\mathbf{r}) = (L_x L_y)^{-1} p_z(z)$ , where  $p_z$  is the marginal density function for the  $z$  coordinate of a scatterer. Computing the average in Eq. (1) over the

\* matthew.foreman@ntu.edu.sg

transverse coordinates in the limit  $L_x, L_y \rightarrow \infty$  yields the delta function  $\delta(\mathbf{q}_\perp)$ , where  $\mathbf{q}_\perp = \mathbf{q} - \mathbf{q} \cdot \hat{\mathbf{z}}$  [14]. This delta function enforces the standard optical memory effect condition  $\mathbf{q}_\perp = \mathbf{0}$ . Averaging over the  $z$  coordinates of the scatterers yields the characteristic function of  $p_z$ , which attains a maximum at  $q_z = 0$  regardless of the form of  $p_z$ . Importantly, the memory effect condition  $\mathbf{q}_\perp = \mathbf{0}$  does not imply  $q_z = 0$ . Thus, while  $\mathbf{q}_\perp = \mathbf{0}$  is a necessary condition for  $C_{ijuv} \neq 0$ , the magnitude of  $C_{ijuv}$  is anisotropic over the set of allowed wavevector combinations, with a maximum attained at  $q_z = 0$ .

The set of wavevectors satisfying  $q_z = 0$  is non-trivial, but can be visualized by considering a simple, hypothetical experiment. Suppose that the slab is illuminated in succession by two plane waves  $E_i$  and  $E_u$  whose wavevectors  $\mathbf{k}_i$  and  $\mathbf{k}_u$  are related by a transverse tilt  $\Delta\mathbf{k}_\perp = \mathbf{k}_{u\perp} - \mathbf{k}_{i\perp}$ . The scattered field in the direction  $\mathbf{k}_j$  under illumination by  $E_i$  will be correlated with the scattered field in the direction  $\mathbf{k}_v$  under illumination by  $E_u$  provided that the scattered wavevectors are related by the same transverse tilt, i.e.,  $\mathbf{k}_{v\perp} - \mathbf{k}_{j\perp} = \Delta\mathbf{k}_\perp$ . Since  $|k_z| = \sqrt{k^2 - |\mathbf{k}_\perp|^2}$ , where  $k = 2\pi/\lambda$  and  $\lambda$  is the wavelength, the additional constraint  $q_z = 0$  then requires

$$\begin{aligned} s_i \sqrt{k^2 - |\mathbf{k}_{i\perp}|^2} - s_j \sqrt{k^2 - |\mathbf{k}_{j\perp}|^2} \\ - s_u \sqrt{k^2 - |\mathbf{k}_{i\perp} + \Delta\mathbf{k}_\perp|^2} \\ + s_v \sqrt{k^2 - |\mathbf{k}_{j\perp} + \Delta\mathbf{k}_\perp|^2} = 0, \end{aligned} \quad (3)$$

where, for example,  $s_i = \text{sgn}(k_{iz})$ , and the signs  $s_i, s_j, s_u$  and  $s_v$  depend on the nature of the experiment. If, for example, the incident plane waves both propagate in the positive  $z$  direction and the scattered fields are measured in reflection, then  $(s_i, s_j, s_u, s_v) = (1, -1, 1, -1)$ . For fixed  $\mathbf{k}_{i\perp}$  and  $\Delta\mathbf{k}_\perp$ , Eq. (3) can be viewed as a non-linear equation for the transverse measurement direction  $\mathbf{k}_{j\perp}$ . Solutions lie on a curve of maximally-correlated scattering directions in Fourier space. When  $\mathbf{k}_j$  does not satisfy Eq. (3), the magnitude of  $C_{ijuv}$  is reduced, but does not necessarily vanish. The rate at which  $C_{ijuv}$  decreases away from  $q_z = 0$  is determined by the characteristic function of  $p_z$ . If, for example,  $p_z(z) = L_z^{-1} \text{rect}(z/L_z)$ , then  $C_{ijuv} \sim \text{sinc}(q_z L_z)$ . In general, correlations remain significant over a non-zero range of  $q_z$ , whose width is inversely related to the slab thickness.

To demonstrate the anisotropy of  $C_{ijuv}$ , we simulate scattering of plane waves by the slab of scatterers described above. We set  $\lambda = 500$  nm and define a slab with size  $L_x = L_y = 1000\lambda$  and  $L_z = 10\lambda$  containing  $N = 1000$  scatterers with positions sampled uniformly over the slab volume. For an incident plane wave  $E_i$ , we compute the scattered field at an arbitrary point  $\mathbf{r}$  away from the slab by

$$E_s(\mathbf{r}) = \sum_{p=1}^N \frac{\exp(ik|\mathbf{r} - \mathbf{r}_p|)}{k|\mathbf{r} - \mathbf{r}_p|} E_i(\mathbf{r}_p). \quad (4)$$

The form of the scattered field in Eq. (4) is generally appropriate for  $\mathbf{r}$  in the far field of each scatterer [17] and implies a single scatterer scattering cross section of  $\sigma = 4\pi/k^2$ , and thus a mean free path  $l = L_x L_y L_z / (\sigma N) \gg L_z$ , placing the slab firmly in the single scattering regime. We calculate the scattered field in the planes  $z_m^\pm = \pm(L_z/2 + \delta)$ , with  $\delta > 0$  (set to  $5\lambda$  in our simulations) chosen to ensure that  $z = z_m^\pm$  is in the far field of the medium, over a transverse window centered at the origin and of extent  $1000\lambda$  in each transverse direction. The angular spectrum representation of the scattered field is then found by taking the Fourier transform of the scattered field over the transverse window. The window size was chosen to capture a large number of speckles, ensuring good resolution in the Fourier domain. In addition, full angular coverage in the Fourier domain is achieved by sampling the field over the transverse window at the Nyquist rates  $\Delta x = \Delta y = \lambda/2$ . Given our parameters, the resulting angular spectra are arrays of size  $2000 \times 2000$  with  $k_x$  and  $k_y$  spanning from  $-k$  to  $k$ .

Scattered angular spectrum arrays  $\tilde{E}_j$  and  $\tilde{E}_v$  are first computed for incident plane waves  $E_i$  and  $E_u$  respectively, with incident transverse wavevectors  $\mathbf{k}_{i\perp} = (-0.6, -0.4)^T k$  and  $\mathbf{k}_{u\perp} = (-0.45, -0.15)^T k$ , corresponding to  $\Delta\mathbf{k}_\perp = (0.15, 0.25)^T k$ . This particular wavevector shift corresponds to a pixel shift of  $(\Delta r, \Delta c) = (250, 150)$  rows and columns in our arrays. To facilitate computation of field correlations, we first align the angular spectra by carefully cropping  $\tilde{E}_j$  and  $\tilde{E}_v$ . Since  $\Delta r, \Delta c > 0$ , we remove the top  $\Delta r$  rows and final  $\Delta c$  columns of  $\tilde{E}_j$ , and the bottom  $\Delta r$  rows and first  $\Delta c$  columns of  $\tilde{E}_v$ . The resulting arrays are both of shape  $1750 \times 1850$  and elements at the same array location are those that are expected to be correlated according to the memory effect condition. To quantify the local correlation between the aligned fields, we define a sliding window of size  $n \times n$ , which extracts submatrices  $W_j$  and  $W_v$  of  $\tilde{E}_j$  and  $\tilde{E}_v$  respectively. For each window position, we compute the normalized correlation

$$C = \frac{\text{tr}(W_j^\dagger W_v)}{\sqrt{\text{tr}(W_j^\dagger W_j) \text{tr}(W_v^\dagger W_v)}}, \quad (5)$$

where  $\text{tr}$  denotes the matrix trace and  $\dagger$  is the conjugate transpose operator. We found that  $n = 3$  provides a reasonable compromise between spatial localization of the correlation peak and small-sample statistical fluctuations. Computing  $C$  this way exploits spatial averaging, allowing us to observe the desired anisotropy from a single realization of the scattering medium.

Fig. 1(a) shows  $|C|$  computed for incident plane waves propagating in the positive  $z$  direction, i.e.  $k_{iz}, k_{uz} > 0$ , and  $\tilde{E}_j$  and  $\tilde{E}_v$  measured in the plane  $z = z_m^+$ , i.e. in transmission. The incident transverse wavevectors  $\mathbf{k}_{i\perp}$  and  $\mathbf{k}_{u\perp}$  are depicted by black circles and  $\Delta\mathbf{k}_\perp$  by a white arrow. A bright band where  $|C| \approx 1$  can be seen

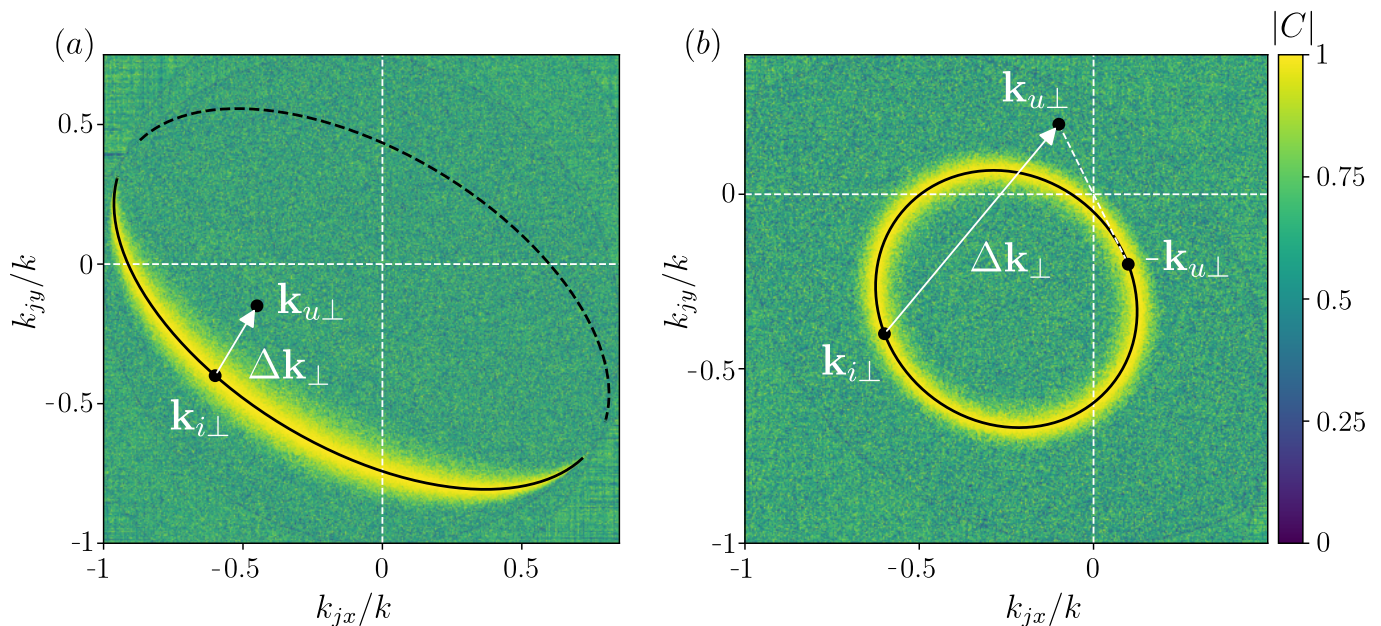


FIG. 1.  $|C|$  calculated as a function of  $\mathbf{k}_j$  as described in the text. Black circles highlight key wavevectors and black lines show theoretical predictions for the curve  $q_z = 0$ . Correlations are calculated between scattered fields (a) in the same plane  $z = z_m^+$  in transmission and (b) between fields evaluated in the planes  $z = z_m^\pm$ , corresponding to two transmitted fields propagating in opposite directions.

to extend across Fourier space, passing through  $\mathbf{k}_{i\perp}$  in a direction approximately orthogonal to  $\Delta\mathbf{k}_\perp$ . The solid black line is the curve  $q_z = 0$ , calculated numerically from Eq. (3) with the choice of signs  $(s_i, s_j, s_u, s_v) = (1, 1, 1, 1)$ , and can be seen to agree well with the simulated data.

We note that the curve  $q_z = 0$  depends on where the scattered field is calculated. If, for example, the scattered fields were instead calculated in the plane  $z = z_m^-$ , i.e., in reflection, the appropriate set of signs in Eq. (3) would be  $(s_i, s_j, s_u, s_v) = (1, -1, 1, -1)$ . As shown by the dashed black line in Fig. 1(a), the corresponding curve for  $q_z = 0$  exhibits opposite curvature to the transmission case.

It is not required that the correlation function be evaluated with two scattered fields in the same plane. In Fig. 1(b), we show  $|C|$  computed with the same  $\mathbf{k}_{i\perp}$  and  $\mathbf{k}_{u\perp}$  as used for Fig. 1(a), but instead with  $k_{iz} > 0$ ,  $k_{uz} < 0$ , and  $\tilde{E}_j$  and  $\tilde{E}_v$  measured in the planes  $z = z_m^+$  and  $z = z_m^-$  respectively. In this case,  $\tilde{E}_j$  and  $\tilde{E}_v$  correspond to fields transmitted through the scattering medium in opposite directions. As before, we see a bright band for which  $|C| \approx 1$  passing through  $\mathbf{k}_{i\perp}$ . In this case, however, the band forms a closed curve. Good agreement is found with the solid black curve computed with Eq. (3) with  $(s_i, s_j, s_u, s_v) = (1, 1, -1, -1)$ .

When correlating fields that transmit through the slab in opposite directions, we find that  $-\mathbf{k}_{u\perp}$  always lies on the curve  $q_z = 0$ . To see why this is the case, note that if  $\mathbf{k}_{j\perp} = -\mathbf{k}_{u\perp}$ , then  $\mathbf{k}_{v\perp} = \mathbf{k}_{j\perp} + \Delta\mathbf{k}_\perp = -\mathbf{k}_{i\perp}$ .  $|C|$  thus represents the degree of correlation between the scattering amplitudes associated with scattering between

the wavevector pairs  $\mathbf{k}_{i\perp} \rightarrow \mathbf{k}_{j\perp} = -\mathbf{k}_{u\perp}$  and  $\mathbf{k}_{u\perp} \rightarrow \mathbf{k}_{v\perp} = -\mathbf{k}_{i\perp}$ . These scattering amplitudes are precisely those that are linked by reciprocity, and thus possess a deterministic relation, regardless of the exact form of the scattering medium [18]. The point  $\mathbf{k}_{j\perp} = -\mathbf{k}_{u\perp}$  is in fact a manifestation of the time-reversed memory effect [3]. Interestingly, the time-reversed peak sits opposite the auto-correlation peak at  $\mathbf{k}_{j\perp} = \mathbf{k}_{i\perp}$  on the curve  $q_z = 0$ .

Finally, we demonstrate that the theory applies equally well to the pseudo-correlation  $C_{ijuv}^P = \langle \tilde{E}_{ji} \tilde{E}_{vu} \rangle$ , which differs from  $C_{ijuv}$  by the absence of a complex conjugation on  $\tilde{E}_{vu}$ . While  $C_{ijuv}^P$  does not exhibit the traditional memory effect, it does exhibit the so-called conjugate memory effect and is non-zero when  $\mathbf{q}_\perp^P = \mathbf{k}_{i\perp} - \mathbf{k}_{j\perp} + \mathbf{k}_{u\perp} - \mathbf{k}_{v\perp} = \mathbf{0}$  [19]. This can be derived following the same argument as for the conventional memory effect given above. The only key difference is that the lack of a complex conjugation gives rise to a different set of signs in Eq. (2). To better understand this effect, note that  $\mathbf{q}_\perp^P = \mathbf{0}$  implies that  $(\mathbf{k}_{i\perp} + \mathbf{k}_{u\perp})/2 = (\mathbf{k}_{j\perp} + \mathbf{k}_{v\perp})/2$ . Thus, given a pair of incident wavevectors  $\mathbf{k}_{i\perp}$  and  $\mathbf{k}_{u\perp}$  with mean value  $\bar{\mathbf{k}}_\perp = (\mathbf{k}_{i\perp} + \mathbf{k}_{u\perp})/2$ , pseudo-correlations exist when  $\mathbf{k}_{j\perp}$  and  $\mathbf{k}_{v\perp}$  are positioned symmetrically about  $\bar{\mathbf{k}}_\perp$ . In other words, rather than thinking of  $\tilde{E}_v$  as a tilted version of  $\tilde{E}_j$ , with regard to pseudo-correlations,  $\tilde{E}_v$  can be thought of as an inversion of  $\tilde{E}_j$  through the point  $\bar{\mathbf{k}}_\perp$ .  $C_{ijuv}^P$  is also anisotropic, with correlations maximized along the

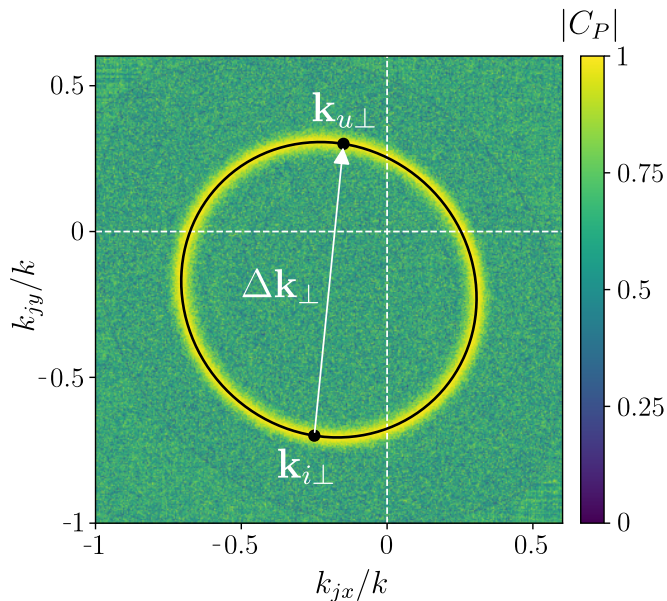


FIG. 2.  $|C^P|$  calculated as a function of  $\mathbf{k}_j$  as described in the text. Black circles highlight key wavevectors and the black line shows the theoretical prediction for the curve  $q_z^P = 0$ . Correlations are calculated between scattered fields in the same plane  $z = z_m^+$  in transmission.

curve  $q_z^P = 0$ , which can be expressed in terms of  $\mathbf{k}_{j\perp}$  as

$$\begin{aligned}
 & s_i \sqrt{k^2 - |\mathbf{k}_{i\perp}|^2} - s_j \sqrt{k^2 - |\mathbf{k}_{j\perp}|^2} \\
 & + s_u \sqrt{k^2 - |2\bar{\mathbf{k}}_{\perp} - \mathbf{k}_{i\perp}|^2} \\
 & - s_v \sqrt{k^2 - |2\bar{\mathbf{k}}_{\perp} - \mathbf{k}_{j\perp}|^2} = 0.
 \end{aligned} \quad (6)$$

Setting  $\mathbf{k}_{i\perp} = (-0.25, -0.7)^T k$  and  $\mathbf{k}_{u\perp} = (-0.15, 0.3)^T k$ , corresponding to  $\mathbf{k}_{\perp} = (-0.2, -0.2)^T k$ , we compute  $C^P$  using Eq. (4), but replacing the conjugate transpose with a matrix transpose. In order to align  $\tilde{E}_j$  and  $\tilde{E}_v$ , we map each element in  $\tilde{E}_v$  to the location

related by an inversion through the array position corresponding to  $\mathbf{k}_{\perp}$ . The values of array elements whose inverted positions would lie outside of the array are set to 0.

Fig. 2 shows  $|C^P|$  in the case  $k_{iz}, k_{uz} > 0$  and  $\tilde{E}_j$  and  $\tilde{E}_v$  calculated in the plane  $z = z_m^+$ , i.e. in transmission. The solid line, computed now from Eq. (6) with signs  $(s_i, s_j, s_u, s_v) = (1, 1, 1, 1)$ , agrees well with the simulated data. We note that while this choice of signs is identical to that used in Fig. 1(a), there are additional sign changes inherent to Eq. (6) compared to Eq. (3) that result in the curve's being closed, rather than open as before. We also note that  $\mathbf{k}_{u\perp}$  now lies on the curve, which highlights a symmetry between the scattering amplitudes associated with scattering between the wavevector pairs  $\mathbf{k}_{i\perp} \rightarrow \mathbf{k}_{u\perp}$  and  $\mathbf{k}_{u\perp} \rightarrow \mathbf{k}_{i\perp}$ . This is not a consequence of reciprocity, but is instead a symmetry unique to single scattering [17].

To conclude, we have shown that memory effect correlations are anisotropic in the Fourier domain. In particular, correlations are maximized when the axial components of the relevant set of wavevectors satisfy a similar equation to that normally satisfied by the transverse components. This phenomenon can be explained straightforwardly in the single scattering regime where the memory effect is most prominent. Numerical simulations support our results and show strong agreement with theoretical predictions. Overall, this work provides a deeper understanding of speckle correlations in random scattering media and reveals that speckle patterns encode additional information about the underlying scatterer distribution than has previously been reported.

## ACKNOWLEDGMENTS

N.B. and M.R.F. were supported by the Nanyang Technological University Grant SUG:022824-00001. M.R.F. acknowledges additional funding from the Institute for Digital Molecular Analytics and Science (IDMxS) under the Singapore Ministry of Education Research Centres of Excellence scheme (EDUN C-33-18-279-V12).

- 
- [1] S. Feng, C. Kane, P. A. Lee, and A. D. Stone, Correlations and fluctuations of coherent wave transmission through disordered media, *Phys. Rev. Lett.* **61**, 834 (1988).
- [2] H. Liu, Z. Liu, M. Chen, S. Han, and L. V. Wang, Physical picture of the optical memory effect, *Photon. Res.* **7**, 1323 (2019).
- [3] R. Berkovits and M. Kaveh, Time-reversed memory effects, *Phys. Rev. B* **41**, 2635 (1990).
- [4] R. Berkovits and M. Kaveh, The vector memory effect for waves, *EPL* **13**, 97 (1990).
- [5] H. Yilmaz, C. W. Hsu, A. Goetschy, S. Bittner, S. Rotter, A. Yamilov, and H. Cao, Angular memory effect of transmission eigenchannels, *Phys. Rev. Lett.* **123**, 203901 (2019).
- [6] O. Katz, P. Heidmann, M. Fink, and S. Gigan, Non-invasive single-shot imaging through scattering layers and around corners via speckle correlations, *Nat. Photon.* **8**, 784–790 (2014).
- [7] U. Gokay, R. J. Kilpatrick, S. A. R. Horsley, D. B. Phillips, and J. Bertolotti, Explaining and exploiting the radial memory effect in multimode optical fibers, *APL Photonics* **11**, 026107 (2026), [https://pubs.aip.org/aip/app/article-pdf/doi/10.1063/5.0303181/20906752/026107\\_1\\_5.0303181.pdf](https://pubs.aip.org/aip/app/article-pdf/doi/10.1063/5.0303181/20906752/026107_1_5.0303181.pdf).
- [8] H. Yilmaz, M. Kühmayer, C. W. Hsu, S. Rotter, and H. Cao, Customizing the angular memory effect for scattering media, *Phys. Rev. X* **11**, 031010 (2021).

- [9] G. Osnabrugge, R. Horstmeyer, I. N. Papadopoulos, B. Judkewitz, and I. M. Vellekoop, Generalized optical memory effect, *Optica* **4**, 886 (2017).
- [10] R. Zhang, J. Du, Y. He, D. Yuan, J. Luo, D. Wu, B. Ye, Z.-C. Luo, and Y. Shen, Characterization of the spectral memory effect of scattering media, *Opt. Express* **29**, 26944 (2021).
- [11] L. Zhu, J. B. de Monvel, P. Berto, S. Brasselet, S. Gigan, and M. Guillon, Chromato-axial memory effect through a forward-scattering slab, *Optica* **7**, 338 (2020).
- [12] L. V. Amitonova, A. P. Mosk, and P. W. H. Pinkse, Rotational memory effect of a multimode fiber, *Opt. Express* **23**, 20569 (2015).
- [13] N. Byrnes and M. R. Foreman, Random matrix theory of polarized light scattering in disordered media, *Waves Random Complex Media* **36**, 249 (2026).
- [14] N. F. Byrnes, *Random matrix modelling of polarised light scattering in disordered media*, Phd, Imperial College London (2023).
- [15] L. Mandel and E. Wolf, *Optical Coherence and Quantum Optics* (Cambridge University Press, 1995).
- [16] J. Goodman, *Statistical Optics* (Wiley, 1985).
- [17] H. Hulst and H. van de Hulst, *Light Scattering by Small Particles* (Dover Publications, 1981).
- [18] N. Byrnes and M. R. Foreman, Symmetry constraints for vector scattering and transfer matrices containing evanescent components: energy conservation, reciprocity and time reversal, *Phys. Rev. Research* **3**, 013129 (2021).
- [19] T. Kawanishi, Z. L. Wang, M. Izutsu, and H. Ogura, Conjugate memory effect of random scattered waves, *J. Opt. Soc. Am. A* **16**, 1342 (1999).